Studies on LDPE—Cyanoethylated Lignocellulosics Blends Using Epoxy Functionalized LDPE as Compatibilizer

R. R. N. Sailaja

Department of Chemical Engineering, Indian Institute of Science, Bangalore 560012, India

Received 18 June 2004; accepted 2 May 2005
DOI 10.1002/app.22992
Published online in Wiley InterScience (www.interscience.wiley.com).

ABSTRACT: Rubberwood flour and cellulose have been plasticized by cyanoethylation and then blended with low-density polyethylene (LDPE). A small quantity of epoxy functionalized polyethylene i.e., polyethylene-*co*-glycidyl methacrylate (PEGMA) has been added to further enhance the mechanical properties. The mechanical properties were measured according to the standard ASTM methods. SEM analysis was performed for both fractured and unfractured blend specimens. The mechanical properties were improved by the addition of PEGMA compatibilizer. LDPE blends with cyanoethylated wood flour (CYWF) showed higher tensile strength and modulus than cyanoethylated cellulose CYC-LDPE blends. However CYC-LDPE blends exhibited higher relative elongation at break values as compared with the former. The TGA analysis showed lowering of thermal stability as the filler content is increased and degradation temperature of LDPE is shifted slightly to lower temperature. DSC analysis showed loss of crystallinity for the LDPE phase as the filler content is increased for both types of blends. Dielectric properties of the blends were similar to LDPE, but were lowered on adding PEGMA. © 2006 Wiley Periodicals, Inc. J Appl Polym Sci 100: 219–237, 2006

Key words: blends; cyanoethylated; mechanical properties; wood flour; LDPE; thermograms

INTRODUCTION

The use of renewable natural bioploymers as components in blends with synthetic polymers has been the focus of the study for the past three decades. Wood is an excellent reinforcing material, which can be used to make a variety of structural components. However owing to the shortage of high quality wood, efforts to use softwood, wood residues, and sawdust are being looked into. These can be chemically modified to develop extrudable wood products. This can be done by thermoplasticization of wood by etherification, cyanoethylation, esterification, or by grafting reactions. Thus, by these processes, wood can then be blended with thermoplastics like low-density polyethylene (LDPE). The thermoplasticization of wood has been thoroughly reviewed by Shiraishi.[1] However, a blend of LDPE with wood is not compatible, owing to the inherent differences in their polar nature. The interfacial adhesion between lignocellulosic materials like wood and cellulose with LDPE can be improved by the addition of coupling agents or by functionalizing of the blend components.[2,3] Tensile strength and elongation at break values have been enhanced by the addition of coupling agent and elastomeric compatibilizer for wood flour-LDPE blends.[4–9] Cyanoethylated sisal fibers in hybrid composites showed improved mechanical properties than untreated fibers.[10] However, there are no records of cyanoethylated wood or cellulose blends with LDPE. The present study deals with blends of LDPE and cyanoethylated lignocellulosics i.e., rubberwood and cellulose. Cyanoethylation imparts thermoplasticity to wood and cellulose and thereby facilitates their processability during extrusion. To improve the compatibility between LDPE and modified wood/cellulose, a small quantity of epoxy-functionalized LDPE i.e., poly (ethylene-*co*-glycidyl methancrylate) (PEGMA) has been added to the blend.

EXPERIMENTAL

Materials

LDPE (Grade 24FS040 with MFI 4 g (10 min)$^{-1}$ from IPCL, Vadodara, India) was used for blending with cellulose (S.d. Fine Chem. Bangalore, India). Chips of rubber wood flour i.e., Hevea Brasiliensis were milled in a Pulverisette 14 of Fristch Inc fitted with 0.2 mm sieve, which was kindly donated by Institute of Wood Science and Technology, Bangalore, India. Acrylonitrile and other chemicals have been obtained from S.d. fine chem. Mumbai India. This monomer was washed with 2% NaOH solution to remove the inhibhitor and

Correspondence to: R. R. N. Sailaja (rrns@chemeng.iisc.ernet.in).

Contract grant sponsor: Department of Science and Technology (DST), New Delhi.

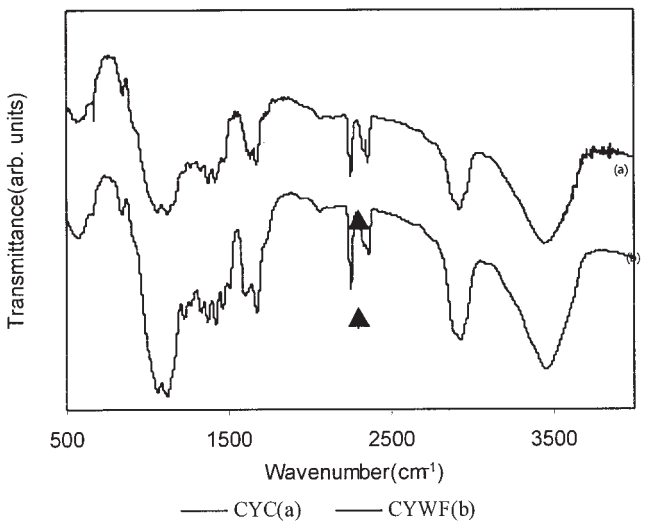

Figure 1 FTIR spectra of cyanoethylated wood and cellulose.

was then rinsed repeatedly with distilled water. The compatibilizer i.e., poly (ehylene-*co*-glycidyl methacrylate) (PEGMA) containing 8 wt % glycidyl methacrylate was purchased from Sigma Aldrich Company.

Cyanoethylation

Cyanoethylation of cellulose and rubberwood was carried out as described by Morita and Sakata.[11] About 20 g of the sample was steeped in 4% sodium hydroxide (NaOH) solution saturated with sodium thiocyanate for 30 min. The slurry was filtered and pressed to 100% NaOH pickup as was carried out by Morita and Sakata.[11] This pretreated sample was then put in 400 mL of washed acrylonitrile and the reaction temperature was maintained at 40°C for 3 h. The product was then neutralized with glacial acetic acid and precipitated in methanol and filtered. The isolated product was washed several times with methanol to remove the by-products. The final product was then vacuum-dried till a constant weight was achieved. The nitrogen content determined by Kjeldahl method was found to be 6.735 and 11.592% for wood and cellulose, respectively. The FTIR spectra for cyanoethylated rubberwood and cellulose obtained by using a Perkin–Elmer model are shown Figure 1. Both spectra clearly indicate the presence of a narrow peak at 2240 cm^{-1} for the nitrile group introduced because of cyanoethylation.

Melt blending

Blends of LDPE, cyanoethylated cellulose/rubberwood, and PEGMA compatibilizer were prepared in varied proportions (by weight) by melt mixing at 210°C in a heated cup fitted with a spiked rotor. Dumb-bell shaped specimens were then molded into standard dies supplied with a minimax molder. Compatibilizer was added in varying proportions by weight w.r.t to the wood flour/cellulose content in the blend.

Mechanical properties of the blend

A Minimax impact (Model CS-183T1079) and a tensile tester (model CS-183TTE) (Custom Scientific Instruments, NJ) were used to measure impact strength and tensile properties, respectively. At least eight specimens were tested for each variation in the composition of the blend. The impact and tensile tests were performed according to ASTM D1822 and ASTM D1708 methods, respectively.

Thermal analysis

Thermogravimetric analysis (TGA) was carried out for the pure materials as well as for the blends, using a Perkin–Elmer Pyris Diamond 6000 analyzer in nitrogen atmosphere. The sample was subjected to a heating rate of 10°C/min in the heating range of 40–600°C, using Al_2O_3 as the reference material. Differential scanning Calorimetry (DSC) of the blend specimens was performed in a Mettler Toledo DSC 822e model. Samples were placed in sealed aluminum cells, using a quantity less than 10 mg and scanning at a heating rate of 10°C/min in the heating range of 25–200°C.

Blend morphology

A scanning electron microscope (SEM) (JEOL, JSM-840A microscope) was used to study the morphology of fractured and unfractured specimens. The specimens were gold sputtered prior to microcopy (JEOL, SM-1100E). The morphology of the unfractured blend specimens was registered after soaking the samples in concentrated sulfuric acid for 10 min.

Dielectric properties

The dielectric properties were measured using a 4192 Impedance analyzer (Hewlett–Packard) at ambient temperature. Test specimens of 2 mm thickness and 1 cm^2 cross section were prepared by injection molding. The samples were coated with silver paint on both sides. Copper wires were fixed as electrodes on each side.

RESULTS AND DISCUSSION

LDPE was separately blended with cyanoethylated wood flour (CYWF) and cyanoethylated cellulose (CYC) using PEGMA compatibilizer. The thermal, me-

TABLE I
Regression Coefficients for Eq. (1)

Mechanical property	Linear terms			Quadratic terms		Interaction terms	Sum of squares means	$\langle r^2 \rangle$	Standard error of estimate
	a_0	a_1	a_2	a_3	a_4	a_5			
RIS (CYC)	0.5955	0.0485	−0.009	−0.0016	0.0001	−0.0005	0.0562	0.77	0.0678
RIS (CYWF)	0.7337	0.0406	−0.015	−0.0015	0.0001	−0.0002	0.0576	0.91	0.0433
RTS (CYC)	0.3747	0.0510	0.0115	−0.0016	−0.0002	−0.0005	0.0492	0.80	0.0591
RTS (CYWF)	0.6576	0.0578	−0.004	−0.0038	−0.0001	0.0002	0.0419	0.76	0.0781
RYM (CYC)	0.7466	−0.065	0.0516	0.0023	−0.0006	−0.0005	0.3575	0.84	0.1364
RYM (CYWF)	2.0674	−0.082	−0.030	0.0040	0.0005	−0.0004	0.2089	0.71	0.1559
REB (CYC)	0.9987	0.0155	−0.031	−0.0006	0.0003	−0.0002	0.0651	0.82	0.0631
REB (CYWF)	0.6719	0.1112	−0.014	−0.0003	0.0001	−0.0001	0.0403	0.93	0.0288

chanical, and dielectric properties of these blends have been examined. To find out the quantitative relationship between response i.e., Y (any relative mechanical property) and the two system variables i.e., filler (x_1) and compatibilizer (x_2) loading, the experimental data was fitted as a second order quadratic eq. (1) parameters for and the ANOVA (analysis of variance) was obtained using sigma plot™ software (version 2).

$$Y = a_0 + a_1x_1 + a_2x_2 + a_3x_1^2 + a_4x_2^2 + a_5x_1x_2 \quad (1)$$

The values of the coefficient a_0–a_5 and $<r^2>$ are given in Table I for each mechanical property for both CYC and CYWF, respectively. The $<r^2>$ values are all above 0.75 (except RYM), indicating that the above equation is a good fit for the experimental property.

Impact strength

Figure 2(a,b) shows the relative (to LDPE) impact strength versus percentage compatibilizer for compatibilized and uncompatibilized CYC-LDPE and CYWF-LDPE blends, respectively. In Figure 2(a), the relative impact strength reduces as CYC loading is increased. For 20 and 30% CYC loading, the impact strength value increases with the addition of PEGMA compatibilizer [Fig. 2(a)]. For higher CYC loading for 40 and 50%, there is a significant increase in relative impact strength values by around 60% for compatibilized blends as compared with uncompatibilized blends [Fig. 2(a)]. In each case, there exists a maximum at 9% compatibilizer beyond which, there is a drop in the impact strength values. CYWF-LDPE blends have shown higher impact strength than CYC-LDPE blends, as observed in Figure 2(b). For 20–50% CYWF loading, there is an optimal compatibilizer content [Fig. 2(b)]. Uncompatibilized blends show low impact strength values that further reduces when CYC or CYWF loading is increased owing to poor adhesion between the filler and matrix. PEGMA efficiently compatibilizes these blends and improves the dispersion of filler in the LDPE matrix. There is a small detrimen-

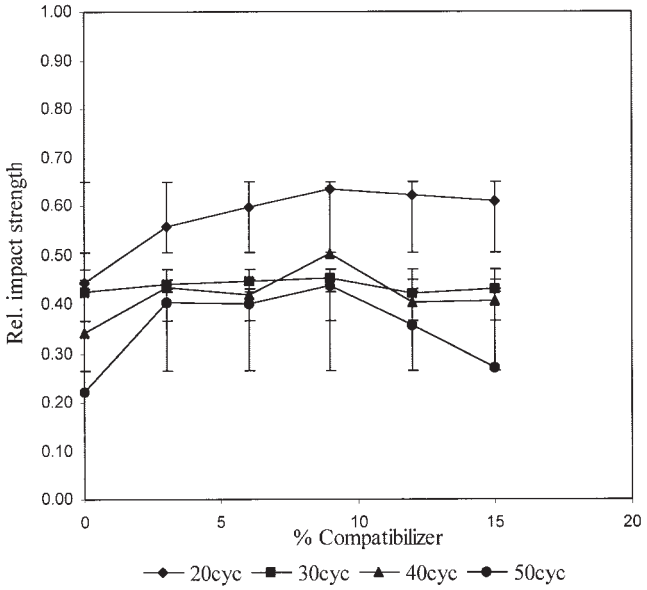

Figure 2 Plot of relative impact strength (RIS) of (a) CYC-LDPE blends versus percentage of compatibilizer and (b) CYWF-LDPE blends versus percentage of compatibilizer.

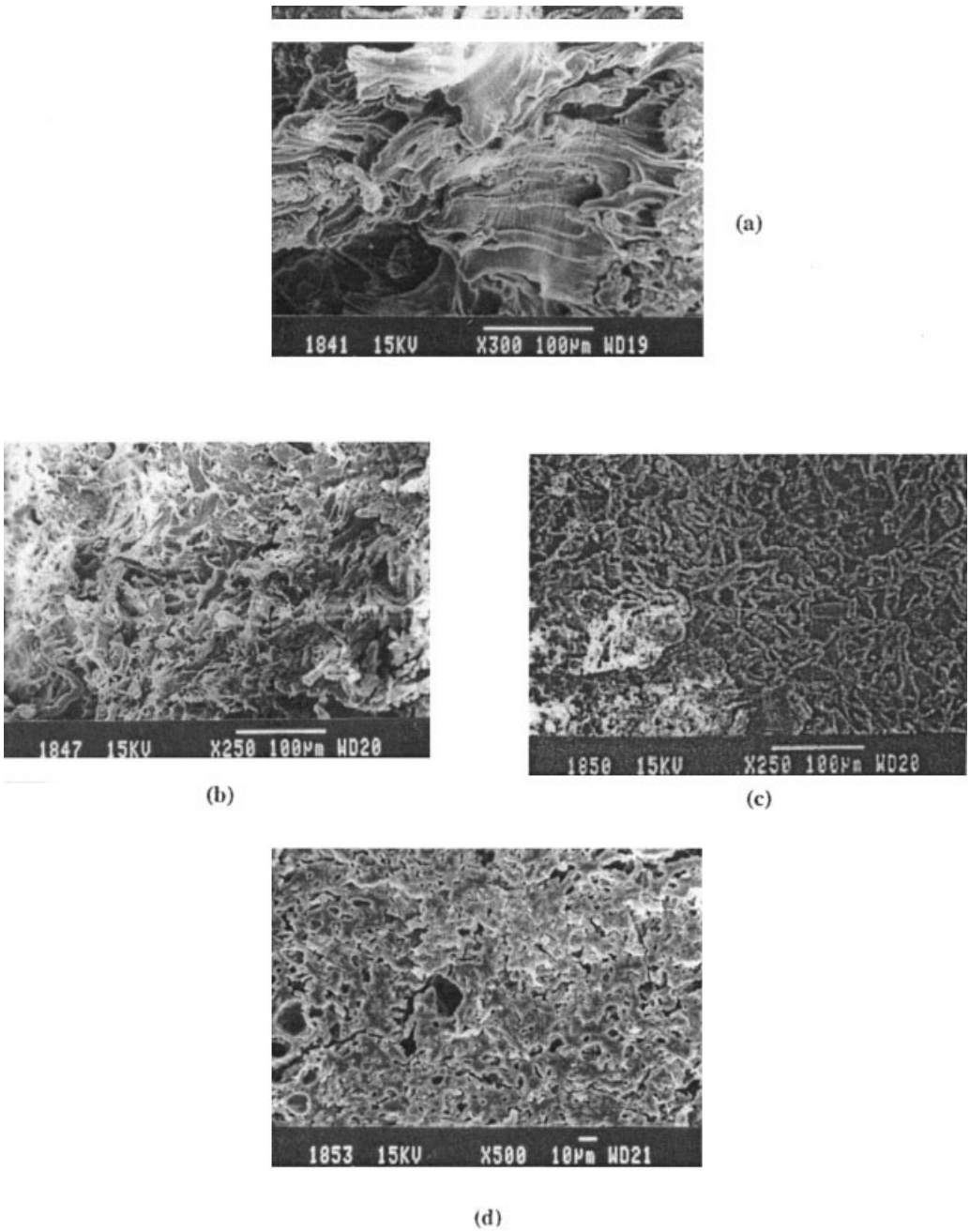

Figure 3 SEM micrographs of impact-fractured blend specimens: (a) 20% CYC and C = 0%, (b) 40% CYC and C = 0%, (c) 40% CYC and C = 3%, and (d) 50% CYC and C = 6%.

tal effect on increasing the compatibilizer content beyond 9% in all samples. It may be due to the accumulation of excess compatibilizer in one of the phases and thus behaves like a ternary blend rather than a compatibilized binary blend.[12] The quadratic model according to eq. (1) for relative impact strength (RIS) values shows a good fit with $<r^2>$ values greater than 0.75 for both CYC and CYWF blends.

The scanning electron micrographs of impact-fractured surfaces are shown in Figure 3 for CYC-LDPE blends. For 20% CYC loading, it can be seen that fracture occurs predominantly by the crazing of the matrix [Fig. 3(a)]. As the quantity of CYC in the blend is low, the matrix is able to withstand the fracture. However, on increasing the CYC loading to 40%, the fracture surface exhibits brittle fracture [Fig. 3(b)]. This is due to lack of stress transfer from the matrix to filler particles. Addition of 3% PEGMA to this blend shows slight plastic deformation of matrix though the mode of fracture is predominantly quasi-brittle [Fig. 3(c)]. For 50% CYC loading [Fig. 3(d)], the brittle fracture that occurs mainly by cavitation though the domain

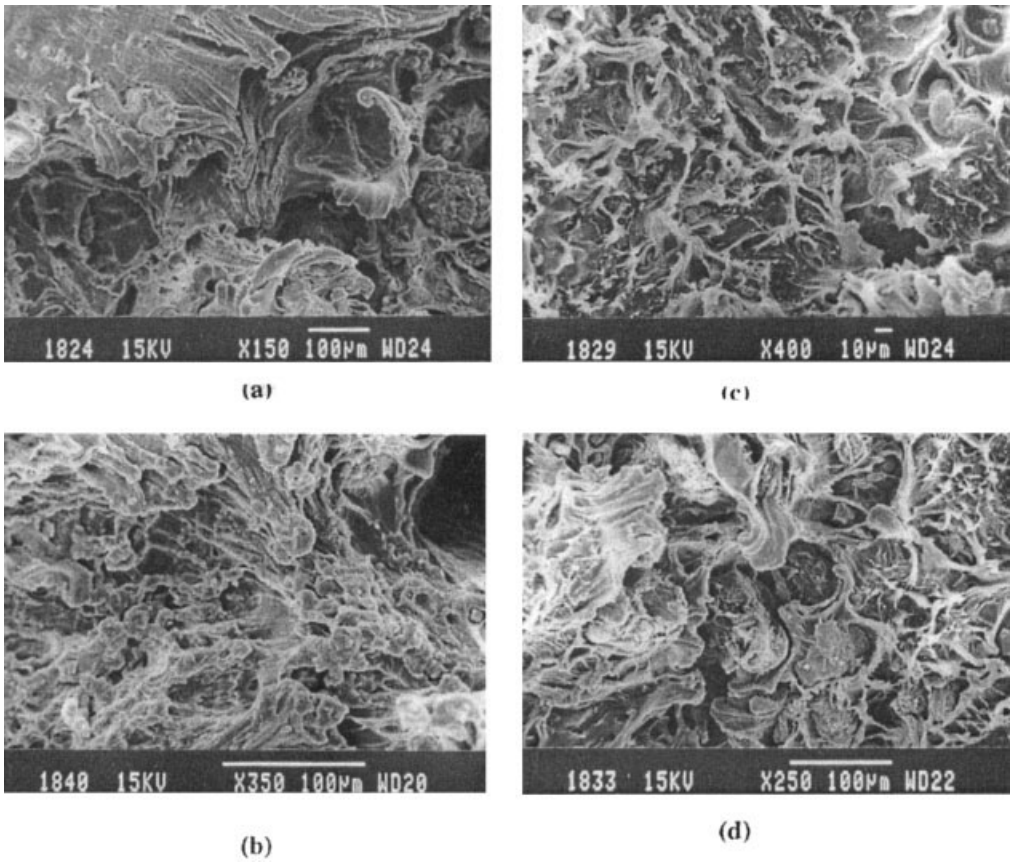

Figure 4 SEM micrographs of impact-fractured blend specimens: (a) 20% CYWF and C = 0%, (b) 20% CYWF and C = 3%, (c) 40% CYWF and C = 0%, and (d) 40% CYWF and C = 3%.

size is smaller due to improved dispersion caused by the addition of compatibilizer.

The SEM micrographs for impact fracture surfaces for CYWF-LDPE blends are shown in Figure 4. For an uncompatibilized blend with 20% CYWF loading, fracture occurred by extensive crazing and matrix deformation. Large holes can be seen due to debonding of agglomerated wood particles [Fig. 4(a)]. Because of differences in the polar nature of matrix and filler, each blend component tries to form separate domains. With the addition of 3% PEGMA [Fig. 4(b)] to the blend, the fracture surface exhibits ductile nature with large plastic deformation of the matrix. Debonding of wood particles from the matrix is also observed showing smaller holes owing to good dispersion of the filler in matrix due to addition of compatibilizer. For higher CYWF loading of 40% [Fig. 4(c) without compatibilizer], the fracture surface is predominantly brittle-characterized by large holes and short fibrils owing to poor adhesion between cyanoethylated wood and LDPE. The impact fracture surface for compatibilized (3% PEGMA) blend shows [Fig. 4(d)] that fracture occurs by plastic deformation of matrix along with pockets of short fibrils giving the appearance of a dimpled network. Because of addition of PEGMA, the particles show resistance to debonding from the LDPE matrix. This causes efficient stress transfer from matrix to filler, which is also reflected in the higher values of relative impact strength as compared with uncompatibilized blends.

Stress–strain curves

Figure 5(a,b) shows the engineering stress–strain curves for CYC-LDPE and CYWF-LDPE blends, respectively. For uncompatibilized blend with 20% CYC loading [curve (a) in Fig. 5(a)], fracture occurs during neck propagation characteristic of quasi-brittle fracture. Increasing the CYC loading to 40% [curve (c) in Fig. 5(a)], a curve typical of brittle fracture and the specimen fails just after yielding with low elongation values. The stress–strain curves for compatibilized (6% PEGMA) blends with 20 and 40% CYC are shown in curves (b) and (d), respectively, in Figure 5(a). Curve (b) shows a marked increase in strain values. The curve indicates an increase in ductility with the presence of a strain-hardening region after yielding. Curve (d) indicates that fracture occurred during neck propagation. At higher filler loading of 40% CYC, the matrix is unable to withstand the draw stress and undergoes quasi-brittle fracture.

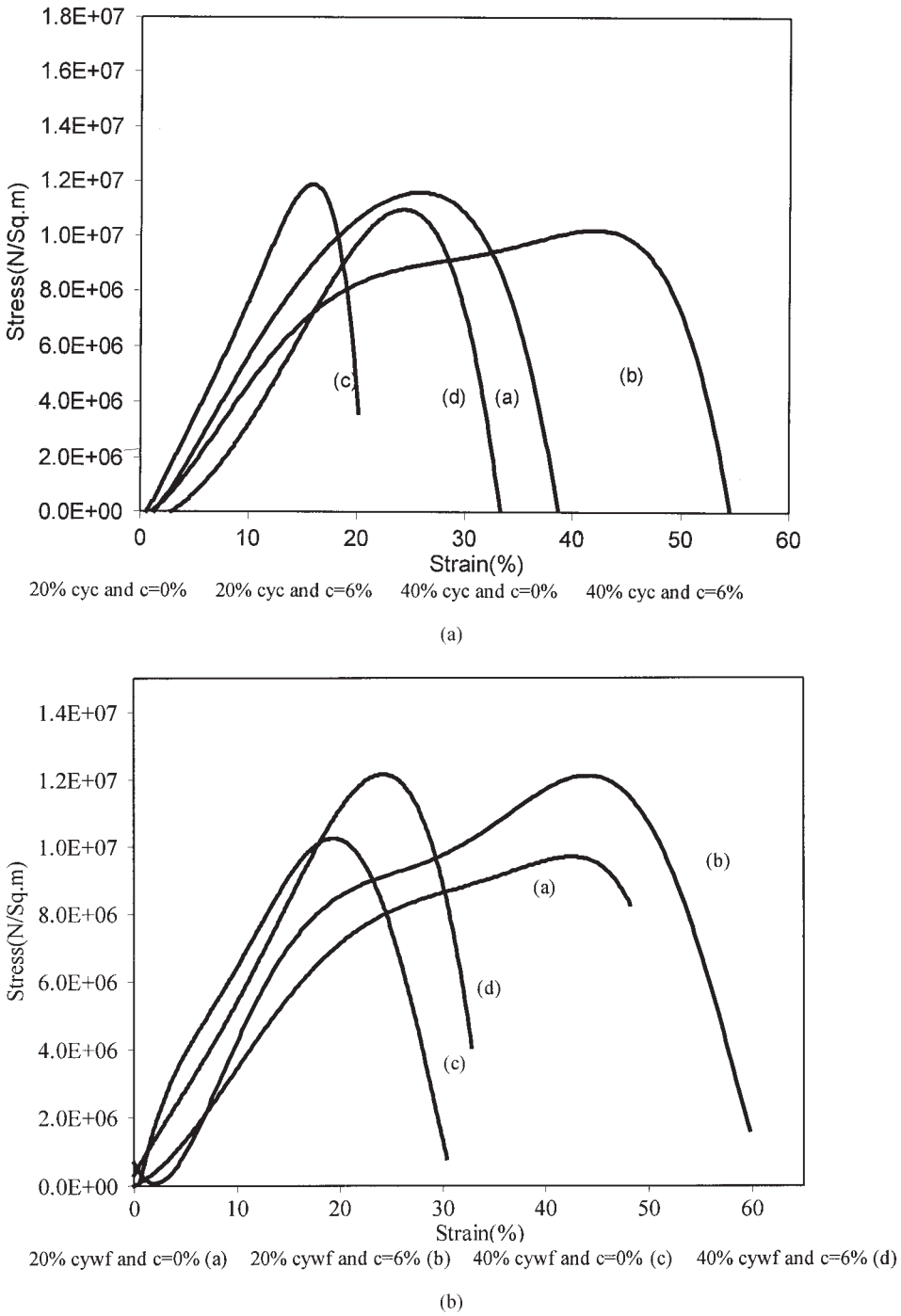

Figure 5 Engineering stress–strain curves for (a) CYC-LDPE and (b) CYWF-LDPE blends.

The stress–strain behavior for CYWF-LDPE blends shows a similar trend as CYC-LDPE blends [Fig. 5(b)]. The curves for uncompatibilized blends for 20 and 40% CYWF [curves (a) and (c)] are typical of quasi-brittle and brittle fracture with lower strain values, respectively. Addition of 6% PEGMA compatibilizer shows significant improvement in both stress and strain values [curves (b) and (d)]. It is interesting to note that CYWF-LDPE blend shows higher strength values than CYC-LDPE blends. It has been observed that there is a strong intermolecular interaction between cellulose and lignin in wood, which results in higher modulus and strength.[13]

Tensile strength

Figure 6(a,b) show the relative (to LDPE) tensile strength of CYC-LDPE and CYWF-LDPE blends, re-

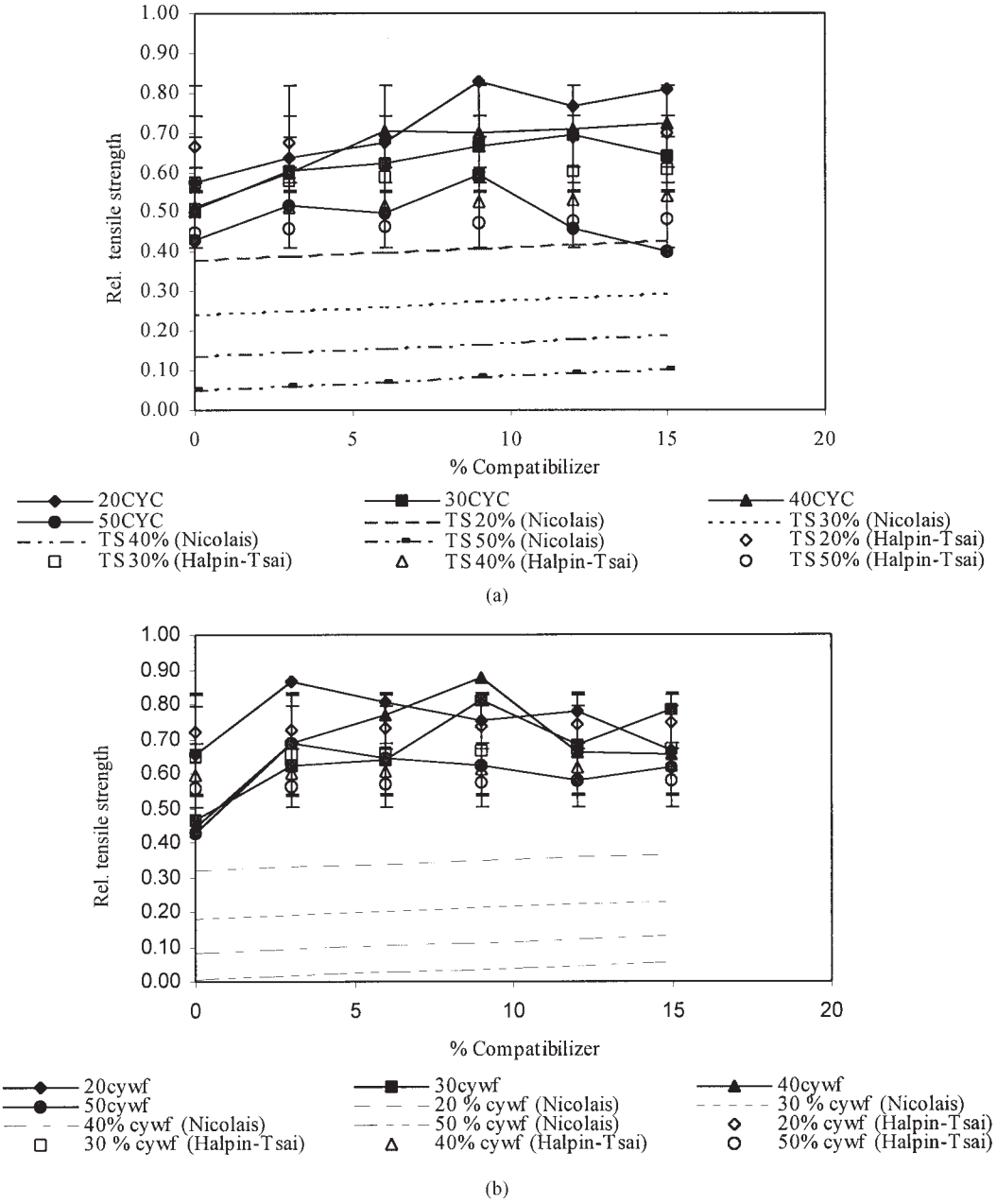

Figure 6 Plot of relative tensile strength versus percentage compatibilizer for (a) CYC-LDPE and (b) CYWF-LDPE blends.

spectively. For both types of blends, the relative tensile strength values are reduced as filler loading is increased. Addition of PEGMA compatibilizer to these, blends, improves the tensile strength owing to better adhesion between the filler and matrix. For 20% CYC loading [Fig. 6(a)], the tensile strength is 85% of that of pure LDPE with 9% PEGMA. For 30 and 40% CYC loading, the relative tensile strength values increases from 0.5 to 0.65 with 6–9% compatibilizer as shown in Figure 6(a). For CYWF-LDPE, a similar trend is observed as shown in Figure 6(b). For 20–40%, the relative tensile strength values are higher than 0.8. For still higher i.e., 50% CYWF loading, tensile strength increases by 60% (for 3% PEGMA) as compared with uncompatibilized blends [Fig. 6(b)].

For both types of blends, a maximum value is reached after which there is a drop in relative (to LDPE) tensile strength (RTS) values. This may be due to the excess compatibilizer, which behaves like a third phase. It has been observed that plasticization of wood itself is supposed to improve mechanical properties as opposed to unmodified wood.[14,15] This may be due to the ease in processing because of plasticization and reduces the degradation of wood. Addition of PEGMA further improves adhesion between filler and matrix, and better stress transfer from matrix to filler

takes place leading to enhanced tensile strength. Nonlinear regression and ANOVA for the experimental data showed good fit with $<r^2>$ values around 0.8 and $P < 0.0001$. The coefficients for eq. (1) are given in Table I.

Two theoretical models have been used to analyze the experimental relative tensile strength values (RTS). These include the Nicolais an Narkis model as given below,

$$\mathrm{RTS} = \frac{\sigma_b}{\sigma_{\mathrm{LDPE}}} = 1 - 1.21\phi_f^{2/3} \tag{2}$$

where $(\sigma_b/\sigma_{\mathrm{LDPE}})$ is the relative tensile strength (i.e., tensile strength of the blend/tensile strength of unfilled LDPE). ϕ_f is the volume fraction of the filler, which was calculated using weight fraction as suggested by Willett.[16]

$$\phi_i = \frac{W_i/\rho_i}{\sum W_i/\rho_i} \tag{3}$$

where ρ_i and W_i are density and weight fraction of component i in the blend. Bulk density values of 0.93 and 0.94 g/cm^3 were used for LDPE and PEGMA, respectively. Modified cellulose and wood flour densities were measured by the standard specific gravity method to be 0.297 and 0.320 g/cm^3, respectively. The calculated theoretical values are also plotted in Figure 6(a,b). The theoretical values are lower than the experimental values obtained. The model assumes that the strength of a particulate composite is determined by the effective area of the matrix, and there is no adhesion between the matrix and filler. This indicates that there is a certain degree of adhesion between filler and matrix even for uncompatiblized blends, which is further improved by the addition of PEGMA. The other model is that of Halpin-Tsai[16] in which the RTS is given by,

$$\mathrm{RTS} = \frac{\sigma_b}{\sigma_{\mathrm{LDPE}}} = \frac{1 + G\eta_T\phi_f}{1 - \eta_T\phi_f} \tag{4}$$

where $\eta_T = R_T - 1/R_T + G$ and $G = 7 - 5v/8 - 10v$.

In eq. (4), R_T is the ratio of filler tensile strength to matrix (LDPE) tensile strength, v is the Poisson's ratio for LDPE and has been taken to be 0.43.[16] In this model, R_T value is adjusted to match the experimental data. R_T value for CYWF-LDPE and CYC-LDPE blends have been found to be 0.45 and 0.3, respectively.

Figures 7 and 8 show the tensile fracture morphology of CYC-LDPE and CYWF-LDPE blends, respectively. The fracture surface of compatibilized (6% PEGMA in Fig. 7(a)) blend with 20% CYC loading is characterized by ductile fracture with extensive shearing and voiding of the matrix owing to good adhesion between filler and matrix. For higher CYC loading of 40%, the specimens fail by brittle fracture [Fig. 7(b)]. However, the filler particles cannot be distinguished even for the uncompatibilzed blend. This suggests that there is certain degree of affinity between the filler and matrix. Cyanoethylation imparts hydrophobicity to a certain extent and thus may show some affinity to the hydrophobic matrix. The fracture surface for the compatibilized (6% PEGMA) blend shown in Figure 7(c) is characterized by quasi brittle fracture with profuse cavitation and bundles of short fibrils. This is typical of mode C fracture suggested by Li et al.[17] For 50% CYC loading (compatibilized with 6% PEGMA), the fracture occurred mainly by extensive cavitation with short single fibrils showing a dimpled surface [Fig. 7(d)].

Figure 8(a) shows the tensile fracture surface for 20% CYWF-LDPE blend with 3% PEGMA. The figure exhibits a fracture surface characterized by extensive crazing with microvoiding and tearing of the matrix. The small size of the voids was created because of debonding of CYWF particles, which absorbs large amount of energy and thereby contributes to high tensile strength values closer to that of LDPE. For 40% CYWF loading [Fig. 8(b)], the uncompatibilized blend exhibits quasi brittle fracture with shearing of the matrix accompanied by cavitation. Addition of 6% PEGMA [Fig. 8(c)] to this blend shows predominant ductile fracture characterized by large matrix yielding with small pockets of brittleness. This is also reflected in the improved tensile strength values [Fig. 6(b)] in contrast to the uncompatibilized blends. At still higher loading i.e., 50% CYWF (6% with PEGMA), extensive microvoiding along with short fibrils typical of brittle fracture is observed [Fig. 8(d)]. The small size of the voids indicate good dispersion owing to improved adhesion between filler and matrix. The RTS values for these blends increases from 0.42 to 0.63 (no compatibilizer).

Tensile modulus

Figure 9(a,b) show the relative (to LDPE) tensile modulus (RYM) for CYC-LDPE and CYWF-LDPE blends, respectively. In both types of blends, the RYM values increases as filler loading owing to the stiffness of filler chains. Compatibilization improves the flexibility by efficiently linking the matrix and filler. In both cases, 6% PEGMA is sufficient to bring the RYM values closer to 1. Increasing the PEGMA loading beyond 6% does not have any effect on the modulus. The substituted cyanoethyl groups impart thermoplasticity and hydrophobicity to the filler material. The epoxy group in PEGMA can react with both unsubstituted hydroxyl group and the nitrile group as suggested in Scheme 1. Nonlinear regression coefficients for RYM

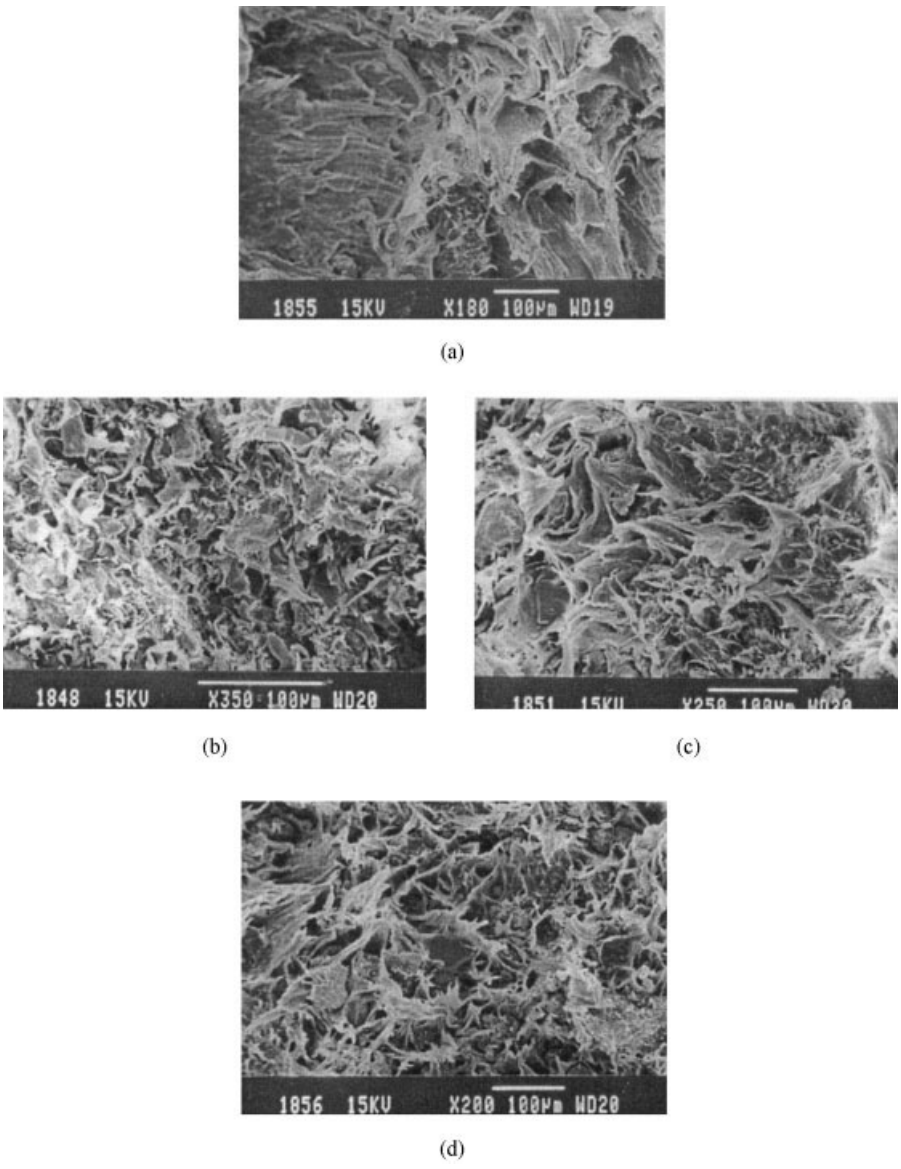

Figure 7 SEM micrographs for tensile-fractured CYC-LDPE blend specimens: (a) 20% CYC and C = 6%, (b) 40% CYC and C = 0%, (c) 40% CYC and C = 6%, and (d) 50% CYC and C = 6%.

values show $<r^2>$ greater than 0.8, which indicates a good fit with the experimental data (coefficients in Table I).

Efforts to correlate experimental values with theoretical values was carried out using the models of Kerner and Halpin-Tsai.[16] The relative modulus (ratio of blend modulus to LDPE modulus i.e., (E_b/E_{LDPE})) according to Kerner's equations is given below.

$$\text{RYM} = \frac{E_b}{E_{\text{LDPE}}} = \left[1 + \left(\frac{\phi_f}{1-\phi_f}\right)\left(\frac{15(1-\nu)}{(8-10\nu)}\right)\right] \quad (5)$$

This equation is widely used when the filler rigidity is more than the matrix. However, this model does not fit the experimental data. This may be due to the inherent assumptions in Kerner's model, which considers that filler will have no effect on matrix performance; thus, not accounting for the strong interfacial adhesion between filler and matrix caused by cyanoethylation of lignocellulosics and compatibilization by PEGMA.

The theoretical values from Halpin-Tsai also included in Figure 9(a,b) were calculated as follows:

$$\text{RYM} = \left(\frac{1 + G\eta\phi_f}{1 - \eta\phi_f}\right) \quad (6)$$

where $\eta = (R-1/R+G)$

The parameter R in the above equation is the ratio of filler modulus to matrix modulus. This model gives a better fit with experimetnal data particularly for lower filler loadings as shown in Figure 9(a,b). The R value

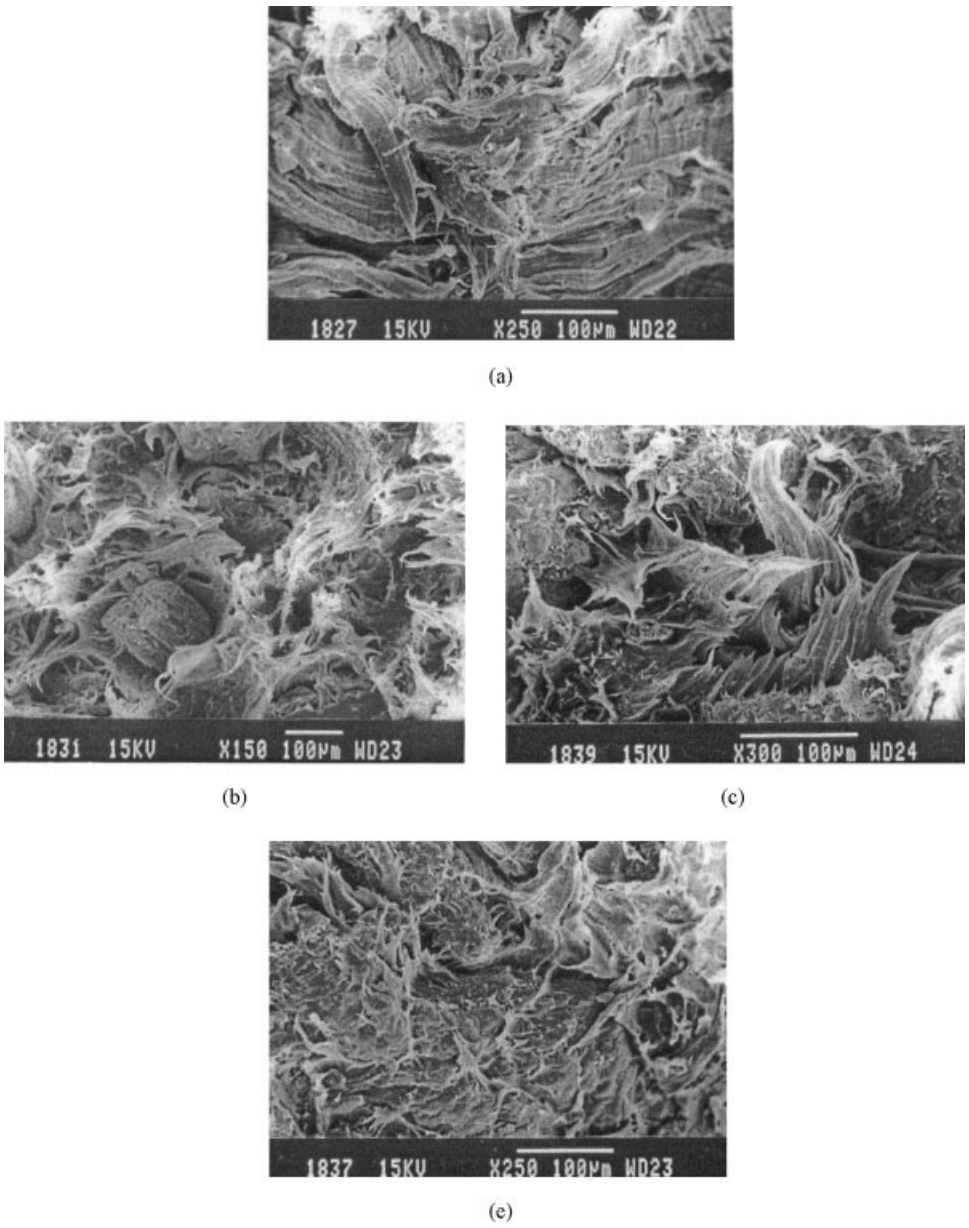

Figure 8 SEM micrographs for tensile fractured CYWF-LDPE blend specimens: (a) 20% CYWF and C = 3%, (b) 40% CYWF and C = 0%, (c) 40% CYWF and C = 6%, and (d) 50% CYWF and C = 6%.

has been obtained to be 1.6 and 2.2 for CYWF-LDPE and CYC-LDPE blends, respectively. It has been speculated[18] that lowering of tensile modulus by reactive compatibilization (Scheme 1) is caused by the fact that PEGMA forms an interphase around CYC or CYWF particles.

Relative elongation of break

The relative (to LDPE) elongation at break (REB) versus compatibilizer content are plotted in Figure 10(a,b) for CYC-LDPE and CYWF-LDPE blends, respectively. The REB values reduce with increase in filler loading from 20–50% because of weak interfacial adhesion between the filler and matrix. However, compatibilized blend shows an improvement in REB values though they are lower than that of unfilled LDPE. This is also observed in the stress–strain curves [Fig. 5(a,b)] where the compatibilzed blends show peak broadening, indicating an improvement in ductility due to improved interfacial adhesion. The nonlinear regression coefficients for REB values for these blends are given in Table I.

The obtained experimental values were compared with the calculated theoretical values of Nielsen model for good adhesion between filler and matrix. The Nielsen's model is given as follows:

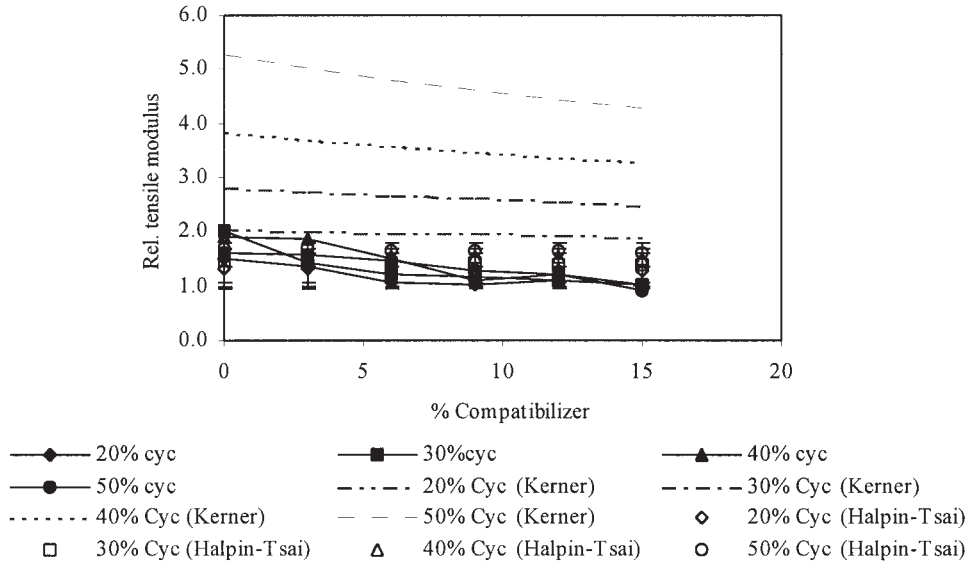

(a)

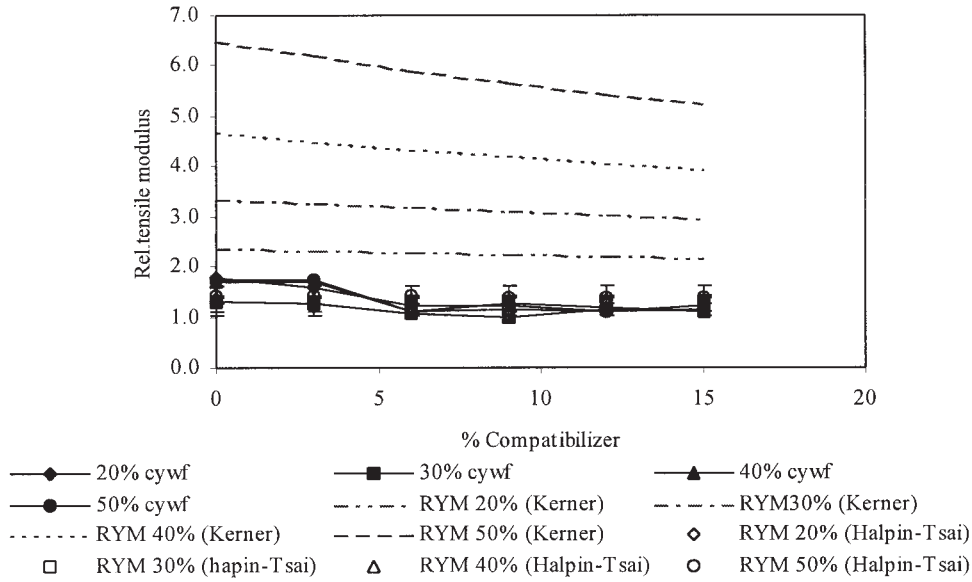

(b)

Figure 9 Plot of relative tensile modulus (RYM) values for the blend versus percentage compatibilizer for (a) CYC-LDPE and (b) CYWF-LDPE blends.

$$\mathrm{REB} = \frac{\varepsilon_b}{\varepsilon_{\mathrm{LDPE}}} = (1 - k\phi_f^{2/3}) \qquad (7)$$

where, ε_b and $\varepsilon_{\mathrm{LDPE}}$ are the elongation at break for the blend and LDPE, respectively. k is an adjustable parameter dependent on filler geometry. The k values for CYC-LDPE and CYWF-LDPE blends have been found to be 0.62 and 0.6, respectively, similar to that obtained by Isabelle et al.[18] For 20% filler loading, 3–6% of PEGMA is essential for the improvement in *REB* values. For 30–50% filler loading, 9–12% compatibilizer gives optimal *REB* values as shown in Figure 10(a, b).

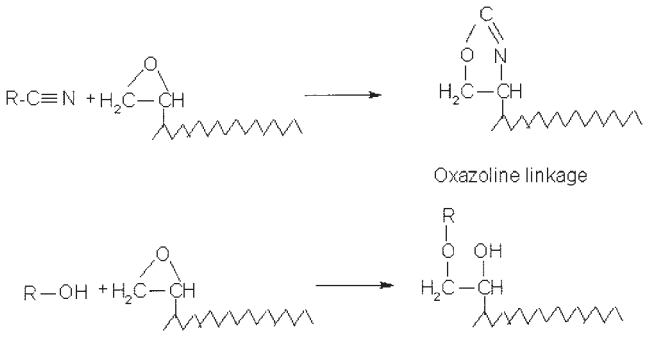

Scheme 1 Possible scheme of reactive blending between the blend components.

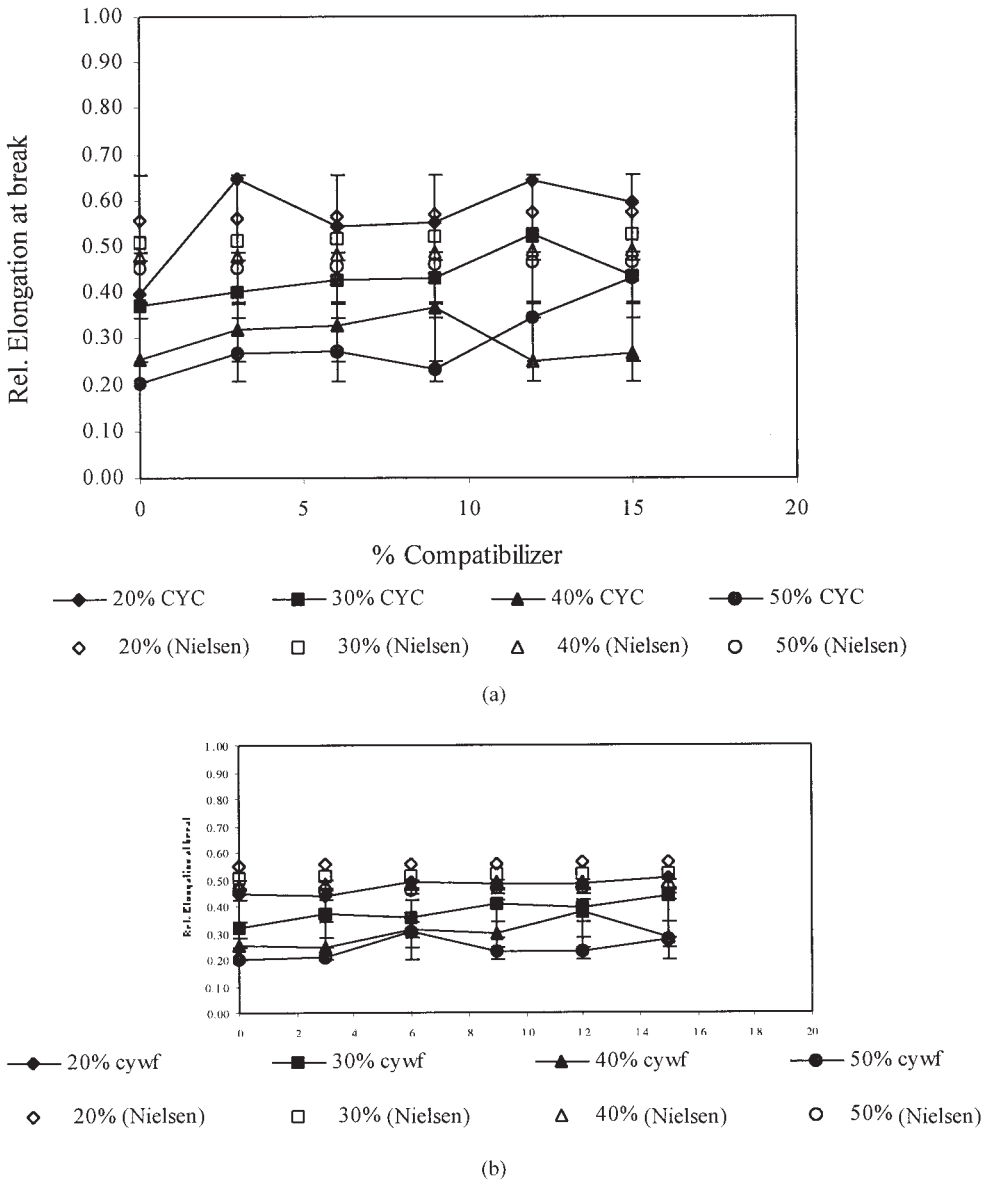

Figure 10 Plot of relative elongation at break (REB) values for the blend versus percentage compatibilizer for (a) CYC-LDPE and (b) CYWF-LDPE blends.

Blend surface morphology

Figure 11 shows blend surface morphology for CYC-LDPE and CYWF-LDPE blends etched with sulfuric acid for 10 min. The two phases are indistinguishable along with small voids for uncompatibilized blend with 20% CYC loading [Fig. 11(a)]. This suggested some affinity between hydrophobic LDPE and CYC. Cyanoethylation imparts hydrophobicity to cellulose or wood by substitution of hydroxyl groups by cyanoethyl groups. Clean etching for the compatibilized [3% PEGMA in Fig. 11(b)], blend has not been observed because of enhanced interaction between filler and matrix, indicated by protruded holes. As result of this strong interfacial adhesion, the matrix offered resistance to the debonding of particles. A similar pattern is observed for higher CYC loading i.e., 40% compatibilized with 3% PEGMA [Fig. 11(c)]. In this case, too small voids accompanied by large deformation of the matrix indicates good dispersion of filler in the matrix.

For 20% CYWF loading compatibilized with 3% PEGMA [Fig. 11(d)], the micrograph shows protruded holes with small voids owing to good dispersion. For 40% CYWF with no PEGMA (Fig. 11(e)), a combination of large holes and small voids are observed in the micrograph. This may be due to the fact that hydrophobicity induced by cyanoethylation improves dispersion only to a certain extent at such high filler

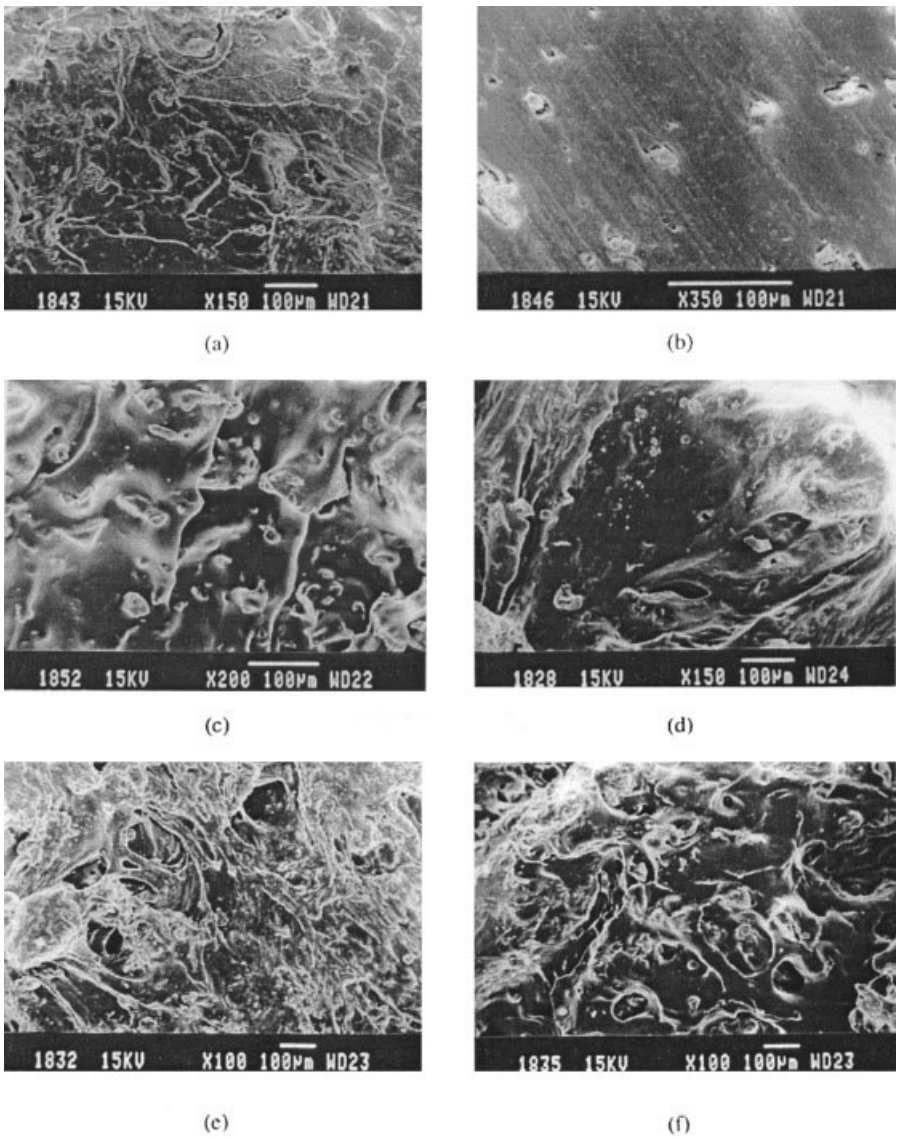

Figure 11 SEM micrographs showing blend morphology for the blend specimens: (a) 20% CYC and C = 0%, (b) 20% CYC and C = 3%, (c) 40% CYC and C = 3%, (d) 20% CYWF and C = 3%, (e) 40% CYWF and C = 0%, and (f) 40% CYWF and C = 3%.

loading. However, a marked improvement in filler dispersion is observed in compatbilized (3% PEGMA) blend as shown in Figure 11(f).

DSC thermograms

Figure 12(a,b) are the DSC thermograms for CYC-LDPE and CYWF blends, respectively. It can be seen that there are three endothermic peaks in curve (a) of Figure 12(a) while in the other curves, there are only two endothermic peaks. However, for CYWF-LDPE blends, there is only asymmetric peak as observed in Figure 12(b). The heat of fusion for the blend samples was obtained by calculating the area under the peaks. The percent crystallinity (X_c) of the LDPE phase was calculated by using the following equation.

$$\%\text{Cyrstallinity}(X_c) = \frac{\Delta H_f}{\Delta H_f^0} \times 100 \quad (8)$$

where, ΔH_f^0 is the heat of fusion for 100% crystalline LDPE and this was taken to be 287.6 mg/mJ.[19]

The peak temperature and percent crystallinity of LDPE phase are given in Table II. The percent crystallinity of LDPE phase in the blends has decreased by CYC or CYWF loading in the blend. Incorporation of CYC and CYWF inhibits close packing of LDPE chains. This indicates that there is a strong interaction between the blend components. The interaction is further enhanced by the addition of PEGMA and this is reflected by a slight reduction in X_c values as compared with uncompatibilized blends as given in Table II. X_c values are lower for CYWF-LDPE blends com-

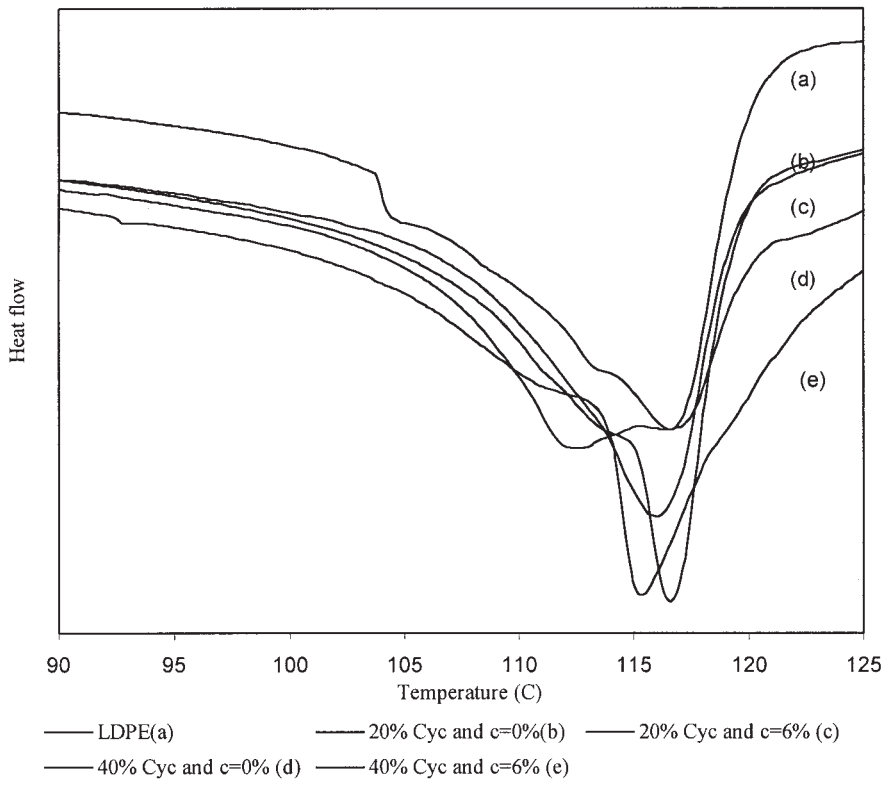

(a)

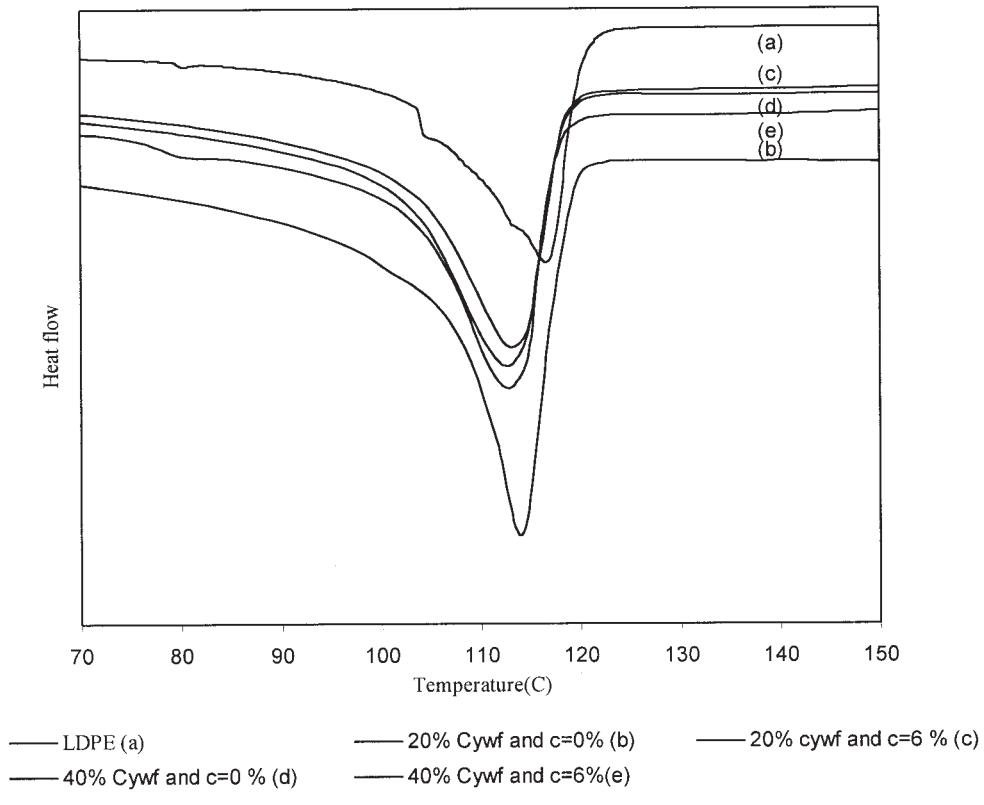

(b)

Figure 12 DSC thermograms for (a) CYC-LDPE and (b) CYWF-LDPE blends.

TABLE II
DSC Analysis for CYC-LDPE and CYWF-LDPE Blends

Blend composition	Peak temp. (T_p) in deg. K	Crystallinity (X_c) (%)
LDPE (Pure)	390.266	33.740
20% CYC (c = 0)	389.630	32.520
20% CYC (c = 6)	389.960	32.520
40% CYC (c = 0)	389.810	28.646
40% CYC (c = 6)	389.076	28.900
20% CYWF (c = 0)	387.802	19.645
20% CYWF (c = 6)	386.480	22.455
40% CYWF (c = 0)	386.260	15.936
40% CYWF (c = 6)	385.557	14.023

pared with CYC-LDPE blends. This may be due to the presence of lignin and hemicellulose in wood, which are amorphous and have strong molecular interactions, which exist between cellulose, and lignin in CYWF as discussed earlier.

Thermogravimetric analysis

Figure 13(a,b) shows that the TGA curves for CYC-LDPE and CYWF-LDPE blends, respectively. The TGA curves for pure LDPE, cellulose, and cyanoethylated cellulose are also included in the plot for the sake of comparison [Fig. 13(a)]. For unmodified cellulose, weight loss begins at 570 K, and the maximum loss in weight occurs at 632 K with reaction going to near completion by 657 K with 80% weight loss. For cyanoethylated cellulose, initial decomposition starts at a lower temperature i.e., 499 K and attains a maximum degradation at 599 K (60% weight loss) when the glucosidic linkage in cellulose breaks down. The maximum degradation temperature of CYC is lower than that of cellulose because of plasticization effect of cyanoethyl groups due to partial substitution of the hydroxyl groups in cellulose or wood flour. These are in agreement with the results obtained by Nada and Hassan.[20] Neat LDPE has the highest thermal stability as compared with the blends. LDPE shows a single stage degradation at 750 K with 80% weight loss occurring due to breakage of C—C backbones. For an uncompatibilized blend with 20% CYC loading, 6% weight loss occurs owing to loss of CYC, and at 750 K, a weight loss of 80% is observed because of thermal decomposition of LDPE. For the compatibilized blend, these temperatures are 572 and 742 K i.e., they are shifted to slightly lower temperature due to increased interaction between the two blend components. For higher CYC loading i.e., 40%, the compatibilized and uncompatibilized blends show a similar trend. In both cases, compatibilized blends show a slightly higher weight loss at different temperatures as compared with uncompatibilized blends. This may be due to decomposition of CYC, which produces free radicals, which can easily attack the hydrogen bonds of LDPE due to its increased accessibility in compatibilized blend.[21]

The TGA plots for neat LDPE, woodflour, and cyanoethylated wood flour is also plotted in the Figure 13(b). The decomposition of untreated wood flour starts at 510 K and reaches a maximum at 620 K with 68% weight loss. By 645 K, there is only 17% of the weight left. This may be due to thermal depolymerization of hemicellulose and cleavage of glucosidic linkage of cellulose near the region of maximum weight loss. Above 675 K, lignin undergoes degradation leading to char formation.[21] The cyanoethylated wood flour shows a maximum weight loss at lower temperature i.e., at 572 K corresponding to 37% weight loss due to plasticization by cyanoethylation. The uncompatibilized blend with 20% CYWF loading shows a three-stage deg-

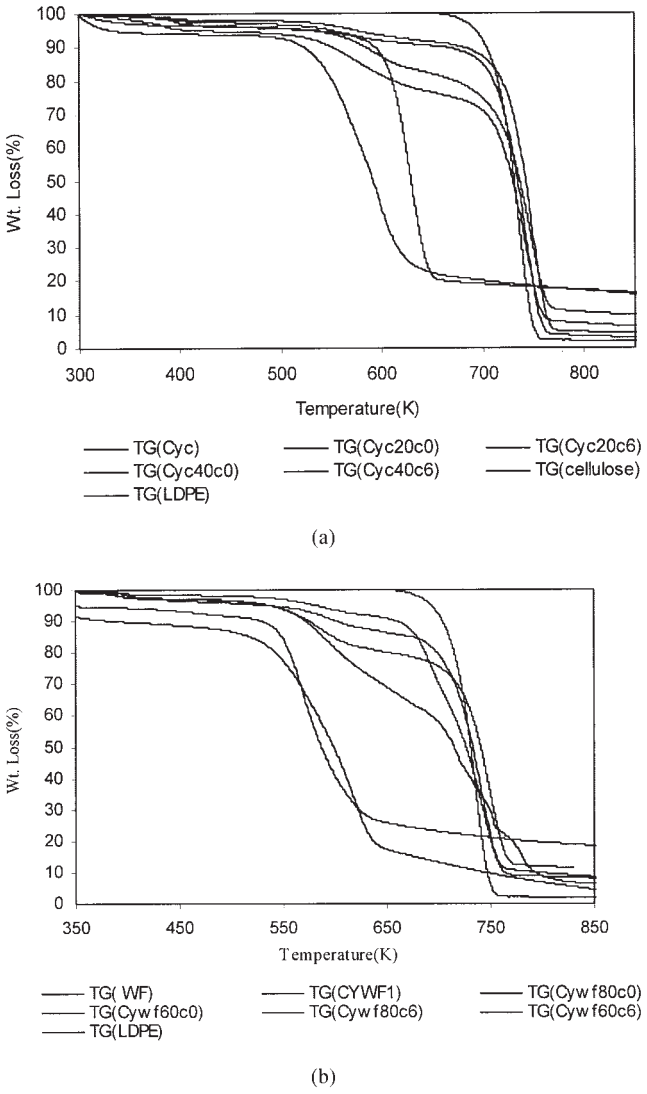

Figure 13 TGA thermograms for (a) CYC-LDPE and (b) CYWF-LDPE blends.

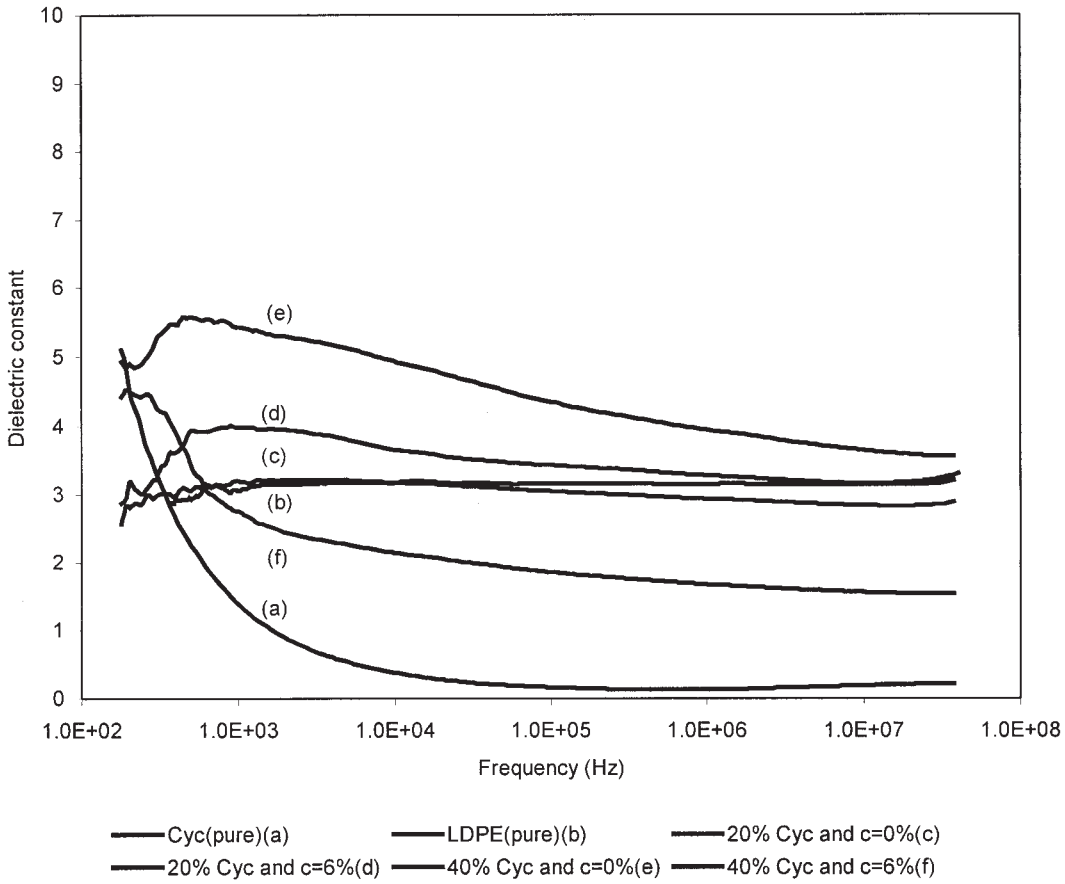

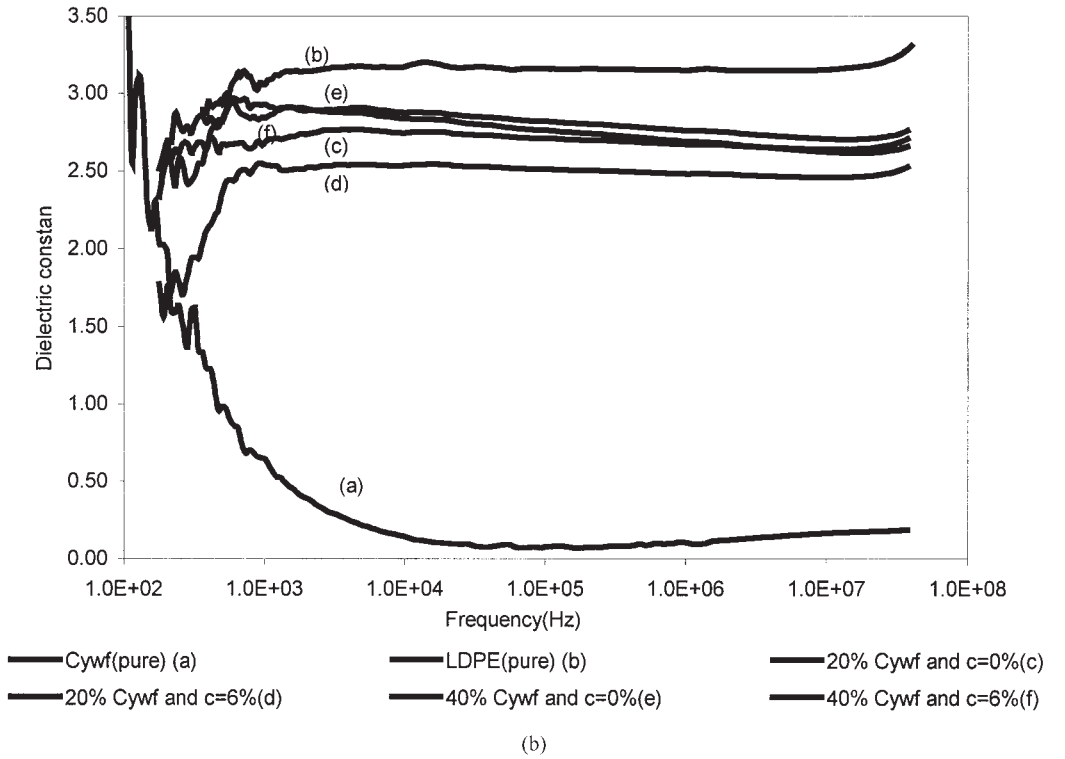

Figure 14 Dielectric constant versus log of frequency (Hz) for (a) CYC-LDPE and (b) CYWF-LDPE blends.

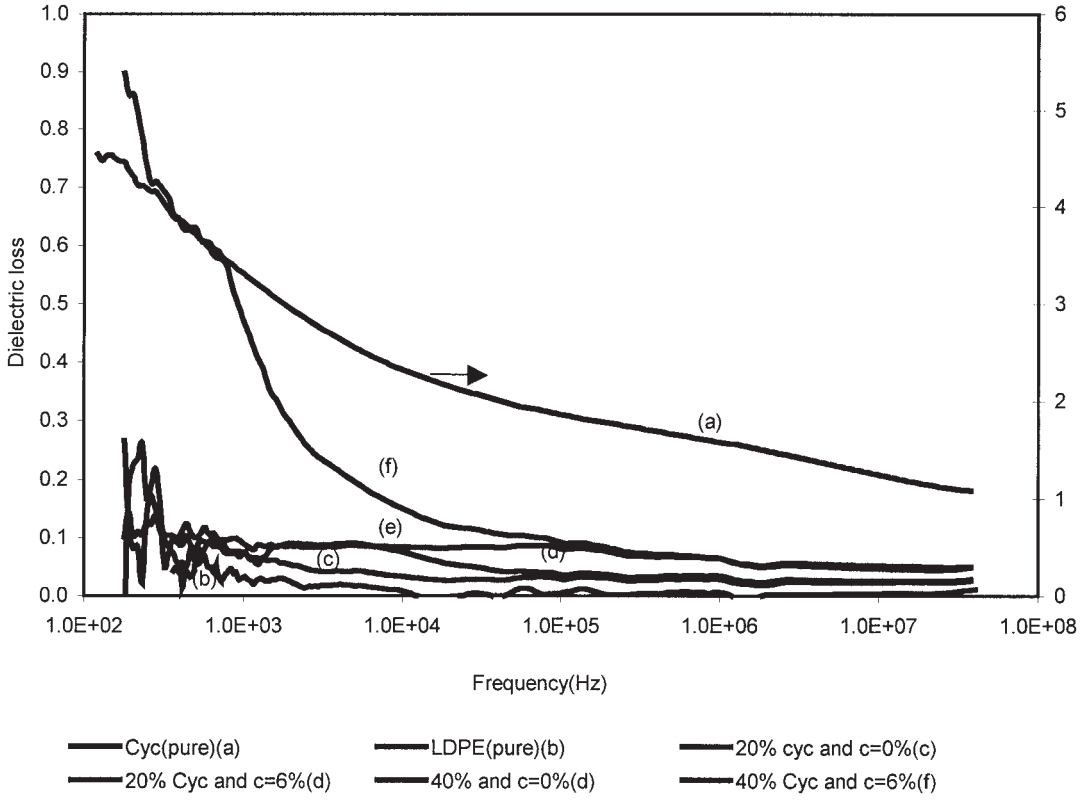

(a)

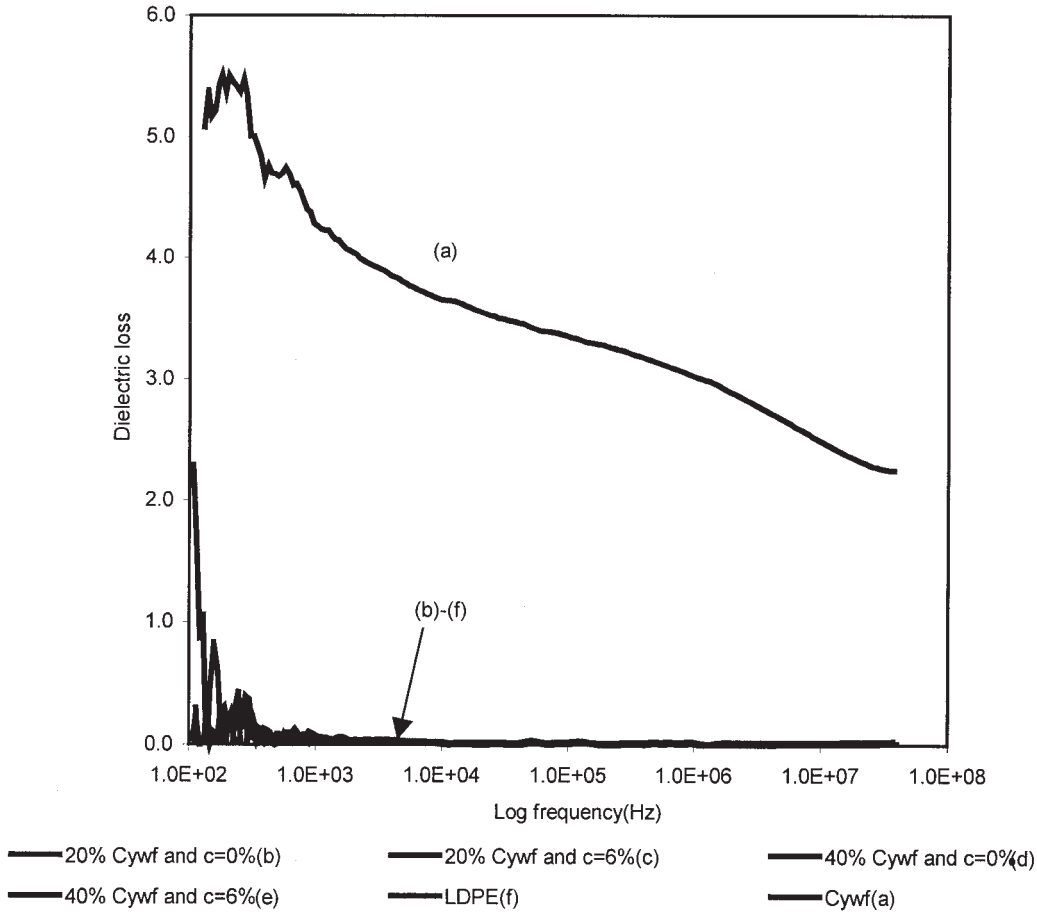

(b)

Figure 15 (a) Dielectric loss factor versus log of frequency (Hz) for CYC-LDPE blends and (b) CYWF-LDPE blends.

radation. The first stage at 594 K (77% wt loss) is due to decomposition of cellulose. The second stage at 696 K is due to lignin degradation and the third stage at 746 K (75% weight loss) is due to thermal decomposition of LDPE. The compatibilized (with 6% PEGMA) blend shows a two stage degradation with no hump at the shoulder as observed for uncompatibilized blend. The region with 9% weight cellulose (cyanoethylated) part of wood is the first stage. The maximum weight loss is at 745 K. The hump observed for uncompatibilized blend at around 696 K is absent for the compatibilized blend. At 696 K, lignin decomposition takes place. However, for a compatibilized blend, the lignin part of cyanoethylated wood may have interacted with epoxy group of PEGMA because of which it may have shifted to a higher temperature, which overlaps with the degradation temperature of LDPE. A similar behavior was observed for 40% CYWF loading with a broad peak at 592 K (16% wt loss) and a shoulder at 586 K (13% weight loss) for the uncompatibilized blend. A two-staged degradation is observed for the compatibilized (6% PEGMA) blend with a small shoulder. The compatibilized blend (6% PEGMA) shows a two-stage degradation at 586 and 753 K with 13 and 70% weight loss, respectively. Thermal degradation is crucial with respect to quality control of blends and setting of blend processing temperature.

Dielectric properties

Figures 14(a) and 14(b) show plots of dielectric constant versus log of frequency for CYC-LDPE and CYWF-LDPE blends, respectively. The dielectric constants for pure materials i.e., LDPE, CYC, and CYWF are also shown in the plots for the sake of comparison. For neat LDPE, the dielectric constant does not vary much with the frequency as it has only atomic and electronic polarization, which are instantaneous. Cyanoethylated lignocellulosics do orient in the applied electric field due to introduction of cyanoethyl groups in cellulose and wood flour. The high values of dielectric constant in the low-frequency region are due to ionic conductivities. For blends having 20% CYC or CYWF loading, their behavior is close to LDPE. For blends, the values of dielectric constant increases slightly (than LDPE) as CYC or CYWF loading increases from 20 to 40% without compatibilizer. The slight increase in dielectric constant may be attributed to the heterogeneous nature of the blend because of addition of cyanoethylated lignocellulosics. This leads to interfacial polarization, which is significant at low frequencies.[22] Further, because of cyanoethylation, hydrophilicity of wood or cellulose is reduced, resulting in reduced orientation polarization, which contributes to the decrease in dielectric constant as compared with untreated blends.[23,24] Another interesting feature, which was observed, was that the compatibilized blends show lower dielectric constant values than uncompatibilized blends. A similar observation has been made by Kim et al.[25] for LDPE/polystyrene blends by adding SEBS compatibilizer. It was argued that on addition of compatibilizer, the size of the dispersed domain reduced, which resulted in reduced charge accumulation as the charges accumulated at the interface can be easily transferred through dispersed phase leading lowering of dielectric constant. The dielectric loss factor versus log of frequency for CYC-LDPE and CYWF-LDPE blends has been plotted in Figure 15(a,b), respectively. Both CYC and CYWF show much higher dielectric loss as compared with LDPE. For blends, the dielectric loss factor for the blends is closer to LDPE in both cases.

CONCLUSIONS

CYWF and CYC were separately blended with LDPE using PEGMA compatibilizer. CYWF-LDPE showed better tensile strength and modulus than CYC-LDPE blends. However, CYC-LDPE showed an increase in ductility leading to enhanced values of REB. TGA analysis showed enhanced interaction between cyanoethylated lignocellulosics and matrix, resulting in the slight lowering of peak temperatures for compatibilized blend. DSC analysis showed loss of crystallinity for LDPE phase because of the addition of the filler, which was further reduced by PEGMA addition, which efficiently links the two immiscible phases and thereby inhibits the close packing of chains. Dielectric measurements for the blend specimens showed values similar to that of LDPE and increased with increased filler content, particularly in the lower frequencies. Enhanced dispersion filler in matrix showed lowering of dielectric constant for compatibilized blends.

References

1. Shiraishi, N. In Wood and Cellulosic Chemistry; Hon, D. N. S., Shiraishi, N., Eds.; Marcel Dekker: New York, 1991.
2. Gaylord, N. U.S. Pat. 3,645,939 (1972).
3. Goettler, L. A. Polym Compos 1983, 4, 249.
4. Oksman, K.; Lindberg, H. J Appl Polym Sci 1998, 68, 1845.
5. Liao, B.; Huang, Y.; Cong, G. J Appl Polym Sci 1997, 66, 1561.
6. Raj, R. G.; Kokta, B. V. ANTEC Conf Proc 1991, 37, 1883.
7. Oaksman, K.; Lindberg, H.; Holmgren, A. J Appl Polym Sci 1998, 69, 201.
8. Farid, S. J.; Kortschot, M. T.; Spelt, J. K. Polym Eng Sci 2002, 42, 2336.
9. Balasuriya, P. W.; Ye, L.; Mai, Y. M.; Wu, J. J Appl Polym Sci 2002, 83, 2505.
10. Mishra, S.; Mohanty, A. K.; Drzal, L. T.; Misra, M.; Parija, S.; Nayak, S. K.; Tripathy, S. S. Compos Sci Technol 2003, 63, 1377.
11. Morita, M.; Sakata, I. J Appl Polym Sci 1986, 31, 831.
12. Sundararaj, U.; Macosko, C. W. Macromolecules 1996, 28, 2647.
13. Glasser, W. G.; Rials, T. G.; Kelley, S. S.; Dane, V. ACS Symp Ser 1998, 688, 265.

14. Hon, D. N. S.; Chao, W. Y. J Appl Polym Sci 1993, 50, 7.
15. Nair, K. C. M.; Diwan, S. M.; Thomas, S. J Appl Polym Sci 1996, 60, 1483.
16. Willett, J. L. J Appl Polym Sci 1994, 54, 1685.
17. Li, J. X.; Hiltner, A.; Baer, E. J Appl Polym Sci 1994, 52, 269.
18. Isabelle, F.; Micheline, B.; Alain, M. Polymer 1998, 39, 4773.
19. Hatakeyama, T.; Liu, Z. Handbook of Thermal Analysis; Wiley: New York, 1990.
20. Nada, A. M. A.; Hassan, M. L. Polym Degrad Stab 2000, 67, 111.
21. Marcovich, N. E.; Villar, M. A. J Appl Polym Sci 2003, 90, 2775.
22. Paul, A.; Thomas, S. J Appl Polym Sci 1997, 63, 247.
23. Paul, A.; Joseph, K.; Thomas, S. Compos Sci Technol 1997, 57, 67.
24. Oksman, K.; Clemons, C. J Appl Polym Sci 1998, 67, 1503.
25. Kim, T. Y.; Kim, W. J.; Lee, T. H.; Ko, J. W.; Kim, J. E.; Suh, K. S. In Proceedings of IEEE International Conference on Properties and Applications of Dielectric Materials, Nagoya, Aichi, Japan, June 1–5, 2003; Vol. 2, p 634.